

****TITLE****

*ASP Conference Series, Vol. **VOLUME**, **PUBLICATION YEAR***

****EDITORS****

AGN Populations from Optical Identification of *ASCA* Surveys

Masayuki Akiyama

*Subaru Telescope, National Astronomical Observatory of Japan, Hilo,
HI, 96720*

Yoshihiro Ueda

ISAS, Sagamihara, Kanagawa, 229-8510, Japan

Kouji Ohta

Department of Astronomy, Kyoto University, Kyoto, 606-8502, Japan

Abstract. To understand luminous AGNs in the $z < 1$ universe, the *ASCA* AGN samples are the best at present. Combining the identified sample of AGNs from *ASCA* Large Sky Survey and Medium Sensitivity Survey, the sample of hard X-ray selected AGNs have been expanded up to 108 AGNs above the flux limit of $10^{-13} \text{ erg s}^{-1} \text{ cm}^{-2}$ in the 2–10 keV hard X-ray band. We discuss the fraction of absorbed AGNs in the hard X-ray selected AGN sample, and nature of absorbed luminous AGNs.

1. Introduction : Importance of a Bright Hard X-ray AGN sample

The fraction of absorbed AGNs, especially luminous absorbed AGNs, is one of a big issue in understanding the true number density of active nuclei in the universe. Recently many candidates of absorbed luminous AGNs are found in AGN surveys in radio, X-ray, and near-infrared wavelengths (e.g., Webster et al. 1995). The discoveries imply that we have been missing significant fraction of nucleus with high activity in traditional optical/UV-selections of AGNs due to absorption to the nucleus. However the fraction of the absorbed AGN in the entire AGN population is not clear. Radio-selected samples are affected by red AGNs with red synchrotron component (Francis et al. 2001), soft X-ray selection is biased against heavily absorbed AGNs (Kim & Elvis 1999), and 2MASS-selected red AGNs are limited in the low redshift universe (Cutri et al. in this volume).

In order to construct a complete sample of AGNs less biased against absorption to nucleus, we conduct optical follow-up observations for *ASCA* Large Sky Survey (hereafter ALSS; Ueda et al. 1999) and *ASCA* Medium Sensitivity Survey (hereafter AMSS; Ueda et al. 2001) in the hard X-ray band. Hard X-ray emission can penetrate the obscuring matter of absorbed AGNs and is very suitable in searching absorbed AGNs. Using 2–10 keV hard X-ray emission, we can detect AGNs with X-ray absorption up to hydrogen column density of $10^{22\sim 23}$

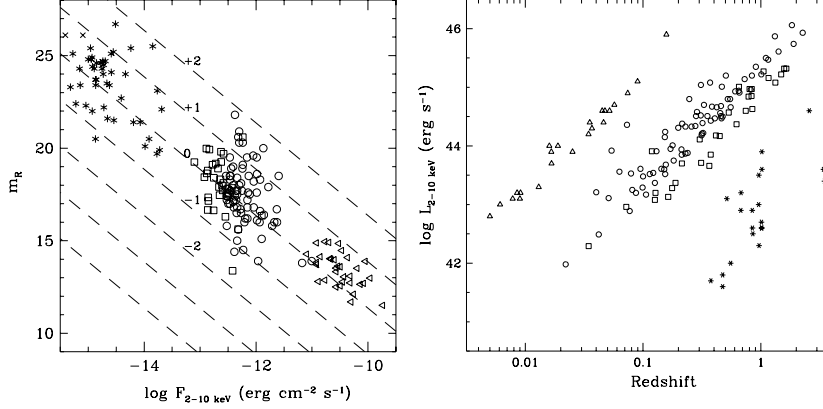


Figure 1. Left) R -band magnitudes of optical counterparts of ALSS (square) and AMSSn (circle) AGNs are plotted as a function of 2–10 keV hard X-ray flux. Dashed lines represent the X-ray to optical flux ratio of $\log f_X/f_V = +2, +1, 0, -1$, and -2 from top to bottom. Triangles and asterisks indicate samples from *HEAO1* A2 (Piccinotti et al. 1982) and *Chandra* survey in HDF-N (Hornschemeier et al. 2001) Right) Hard X-ray luminosities of the hard X-ray selected AGNs plotted as a function of redshift. Same symbols as in the left panel.

cm^{-2} , which corresponds to A_V of $20 \sim 50$ with galactic conversion factor, without bias. ALSS is a survey in a continuous field with 5.4 square degree near the north galactic pole. We selected 34 X-ray sources detected with SIS 2–7 keV significance larger than 3.5σ . The sources are identified with 30 AGNs, 2 clusters of galaxies and 1 galactic star (Akiyama et al. 2000). One X-ray source with hard spectrum is still unidentified, and *Chandra* follow-up observation is planned in Cycle 3. AMSS is a serendipitous source survey based on *ASCA* pointing observations conducted in high galactic latitude region ($|b| > 20^\circ$). We conducted optical follow-up observations for 86 X-ray sources detected with GIS 2–10 keV significance larger than 5.6σ in the northern sky (declination above 20° ; we call AMSSn sample). All of the X-ray sources are identified with 78 AGNs, 7 clusters of galaxies, and 1 galactic star (Akiyama et al. in preparation). In total, we constructed sample of 108 hard X-ray selected AGNs with the flux limit of *ASCA*, about $\sim 10^{-13} \text{ erg s}^{-1} \text{ cm}^{-2}$ in the 2–10 keV band. In Figure 1, we plotted the hard X-ray flux vs. optical magnitude (left) and the redshift vs. luminosity distribution (right) diagrams of ALSS and AMSSn AGNs. The *ASCA* samples are two orders of magnitude brighter and more luminous than the sample of deep *Chandra* and *XMM-Newton* surveys, and consists of luminous AGNs, i.e., QSOs, in the universe below redshift 1. The high completeness of the *ASCA* samples makes us possible to discuss the fraction of absorbed AGNs definitely.

2. Fraction of Heavily Absorbed AGNs

Using the hardness of X-ray spectrum of each source, we can estimate the X-ray absorption to the nucleus in each object. The 0.7–10 keV apparent photon

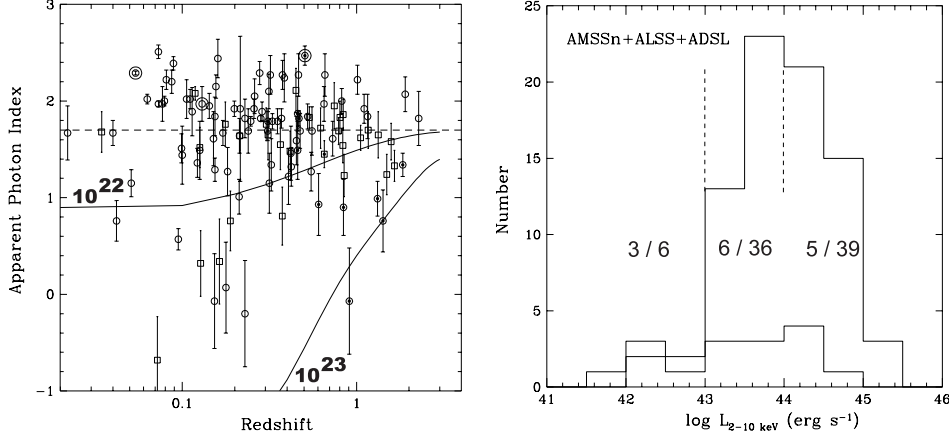


Figure 2. Left) Apparent photon index of ALSS (squares) and AMSSn (circles) AGNs in the 0.7–10 keV hard X-ray band are plotted as a function of redshift. BL Lac objects are marked with large circles. The solid lines show the apparent photon index of power-law continuum with intrinsic photon index of 1.7 absorbed by hydrogen column density of 10^{22} cm^{-2} (top) and 10^{23} cm^{-2} (bottom) at each redshift. AGNs with a faint optical counterpart ($\log f_X/f_V$ larger than 1) are marked with dots. Right) Luminosity distribution of all (thin) and significantly absorbed (thick) AGNs below redshift of 0.6 from combination of AGN samples of ALSS, AMSSn, and ADSL.

index distributions of ALSS and AMSSn AGNs are plotted as a function of redshift in left panel of Figure 2. The upper and lower solid lines in the figure correspond to the apparent photon index of an object with intrinsic photon index of 1.7 and X-ray absorption with hydrogen column density of $\log N_H = 22 (\text{cm}^{-2})$ and $\log N_H = 23 (\text{cm}^{-2})$ at each redshift, respectively. The X-ray sources with apparent photon index smaller than 1 can be regarded as significantly harder than canonical power-law spectra of broad-line AGNs (with photon index of 1.7). They correspond to intermediate redshift AGNs with X-ray absorption of $\log N_H = 22 - 23 (\text{cm}^{-2})$ and high-redshift AGNs with absorption of $\log N_H > 23 (\text{cm}^{-2})$. At high-redshift ($z \sim 1$), the apparent photon indexes of highly absorbed objects become close to that of object without absorption, because we observe very high energy photons of the source-frame, which are less affected by absorption than low-energy photons.

Based on the estimated amount of absorption to nucleus, we examine the fraction of absorbed AGNs in the hard X-ray selected AGNs. For simplicity, we limit the sample below redshift of 0.6, and regard AGNs with $\log N_H > 22 (\text{cm}^{-2})$ as significantly absorbed AGNs. It should be noted that at high-redshifts ($z > 0.6$) AGNs with hydrogen column density of $\log N_H = 10^{22-23} (\text{cm}^{-2})$ can not be regarded as significantly absorbed in the current sample. In right panel of Figure 2, the luminosity distribution of the all AGNs and significantly absorbed AGNs from combination of the ALSS, AMSSn, and ASCA Deep Survey in the Lockman Hole (ADSL; Ishisaki et al. 2001) is plotted. The fraction of absorbed AGNs is higher in the lowest luminosity range, but there is no clear deficiency

of absorbed AGN above 10^{44} erg s $^{-1}$, which is observed in the ALSS sample (Akiyama et al. 2000). The fraction of absorbed AGN are 6/36 and 5/39 in the luminosity between 10^{43} erg s $^{-1}$ and 10^{44} erg s $^{-1}$ and in the luminosity above 10^{44} erg s $^{-1}$, respectively. The fraction of absorbed AGNs is higher in the luminosity range below 10^{43} erg s $^{-1}$ (3/6) than in the luminosity range above, but the number of AGNs in the low luminosity range is fairly limited. The fraction of luminous ($L_X > 10^{44}$ erg s $^{-1}$) AGNs with $\log N_H > 22(\text{cm}^{-2})$ in the sample of AGNs without bias up to $\log N_H = 23(\text{cm}^{-2})$ ($\sim 15\%$) is clearly smaller than that expected from the models of cosmic X-ray background (45%; Comastri et al. 1995) or that observed in local low-luminosity Seyfert galaxies (40%; Risaliti et al. 1999).

3. Case studies on absorbed QSOs

The fraction of absorbed QSOs is not as large as expected, but we detected several candidates of absorbed QSOs in *ASCA* surveys. Their counterparts are relatively faint and have larger X-ray to optical flux ratio than normal AGNs (see dotted objects in left panel of Figure 2). Most of high-redshift AGNs with hard X-ray spectra have large X-ray to optical flux ratios. The X-ray to optical flux ratio is similar to those of optically-faint hard X-ray source population found in deep *Chandra* surveys (see left panel of Figure 1; e.g., Alexander et al. 2001), and the *ASCA* optically-faint AGNs can be low-redshift and/or high-luminosity cousin of the *Chandra* population.

Although measured amount of X-ray absorption is large, most of the luminous absorbed QSOs show broad MgII 2800Å or H α 6563Å emission line. The origin of the discrepancy can be 1) broad MgII 2800Å from scattered nuclear light or 2) discrepancy between amount of X-ray photoelectric absorption and optical dust reddening. We show two examples of absorbed QSOs fall in each category.

3.1. An absorbed QSO at $z = 0.65$ with a strong broad MgII 2800Å emission line

AX J131831+3341 is an absorbed radio-quiet QSO at a redshift of 0.65 found in ALSS (Akiyama et al. 2000). Its X-ray luminosity is estimated to be $\sim 10^{45}$ erg s $^{-1}$, which corresponds to the luminosities of QSOs. The observed X-ray spectrum of the object in a 0.7–10 keV band is described by intrinsic absorption with a hydrogen column density of $N_H = 6.0^{+4.4}_{-4.2} \times 10^{21}$ cm $^{-2}$ and an intrinsic photon index of 1.7. The hydrogen column density corresponds to the lower edge of the column density distribution of Seyfert 1.8-1.9 galaxies.

The optical spectrum of the object shows strong emission lines, such as broad MgII 2800Å, narrow [OII] 3727Å, and narrow [OIII] 5007Å, but no broad H β emission line (see right panel of Figure 3). Its small H β -to-[OIII] 5007Å equivalent width ratio is comparable to those of Seyfert 1.8-2 galaxies. Optical and near-infrared images show nuclear and extended components (see left panel of Figure 3). Because the nuclear component has very red $I - K$ color but blue $V - R$ and $R - I$ colors, the nucleus is thought to be absorbed with $A_V \sim 3$ and emerge only in the K -band (Akiyama and Ohta 2001). The amount of absorption is consistent with the amount of X-ray absorption. The optical blue

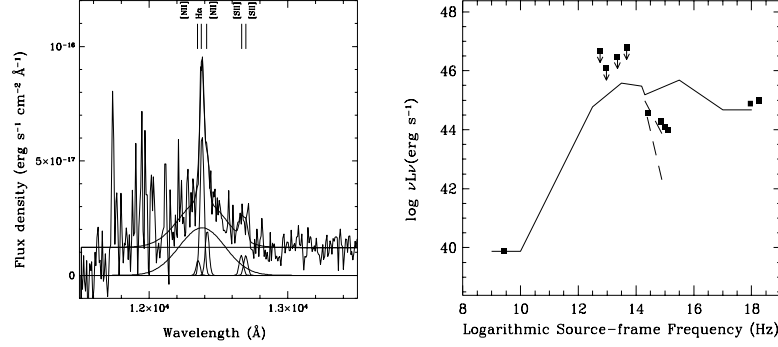


Figure 4. Left) J -band spectrum of AX J08494+4454. The best fit models are also plotted with solid lines. Right) Spectral energy distribution (SED) of AX J08494+4454. Solid line indicates SED of an average radio-quiet QSO (Elvis et al. 1994) and is normalized at the data point observed at 1.4 GHz. Dashed lines represent optical SEDs affected by dust extinction with A_V of 1 mag (upper) and 2 mag (lower).

Acknowledgments. The authors would like to thank ALSS and AMSS members.

References

- Akiyama, M., et al. 2000, ApJ, 532, 700
Akiyama, M., and Ohta, K. 2001, PASJ, 53, 63
Akiyama, M., et al. 2001, PASJ, 52, 577
Akiyama, M., Ueda, Y., and Ohta, K. 2002, ApJ, in press (astro-ph/0111037)
Alexander, D.M., et al. 2001, ApJ, in press (astro-ph/0107450)
Comastri, A., Setti, G., Zamorani, G., and Hasinger, G. 1995, A&A, 296, 1
Elvis, M., et al. 1994, ApJS, 95, 1
Francis P.J., et al. 2001, PASA, in press (astro-ph/0107235)
Hornschemeier, A., et al. 2001, ApJ, 554, 742
Ishisaki, Y., et al. 2001, PASJ, 53, 445
Kim, D., and Elvis, M. 1999, ApJ, 516, 9
Maiolino, R., Marconi, A., and Oliva, E. 2001, A&A, 365, 37
Ohta, K., et al. 1996, ApJ, 458, 57
Piccinotti, G., et al. 1982, ApJ, 253, 485
Risaliti, G., Maiolino, R., Salvati, M. 1999, ApJ, 522, 157
Ueda, Y., et al. 1999, ApJ, 518, 656
Ueda, Y., et al. 2001, ApJS, 133, 1
Webster, R., et al. 1995, Nature, 375, 469